

**This Page Is Inserted by IFW Operations
and is not a part of the Official Record**

BEST AVAILABLE IMAGES

Defective images within this document are accurate representations of the original documents submitted by the applicant.

Defects in the images may include (but are not limited to):

- **BLACK BORDERS**
- **TEXT CUT OFF AT TOP, BOTTOM OR SIDES**
- **FADED TEXT**
- **ILLEGIBLE TEXT**
- **SKEWED/SLANTED IMAGES**
- **COLORED PHOTOS**
- **BLACK OR VERY BLACK AND WHITE DARK PHOTOS**
- **GRAY SCALE DOCUMENTS**

IMAGES ARE BEST AVAILABLE COPY.

**As rescanning documents *will not* correct images,
please do not report the images to the
Image Problem Mailbox.**

Design and Understanding of Anisotropic Conductive Films (ACFs) for LCD Packaging

Myung-Jin Yim and Kyung-Wook Paik

Department of Materials Science and Engineering

Korea Advanced Institute of Science and Technology

373-1, Kusong-dong, Yusong-gu, Taejeon, 305-701, Korea

Phone : 82-42-869-3335, Fax : 82-42-869-3310, E-Mail : kwpaik@sorak.kaist.ac.kr

Abstract

Anisotropic conductive film (ACF) composed of an adhesive resin and fine conductive fillers such as metallic particles or metal-coated polymer balls are key materials for fine pitch chip-on-film (COF) and chip-on-glass (COG) LCD packaging technologies.

To understand and design better quality ACF materials, the theoretical electrical conduction model with physical contact mechanism was simulated and experimentally proved. To understand the contact area changes, two pressure dependent models - 1) elastic/plastic deformation and 2) FEM model-were developed, and experimentally proved by various ACFs fabricated in our laboratory. Experimental variables were applied bonding pressure, number, size, mechanical and electrical properties of nickel powders and Au-coated polymer conductive particles.

It was found that the models were in good agreement with experimental results except at higher bonding pressure realm. In general, as bonding pressure increases, a sharp decrease of contact resistance followed by a constant value is observed after reaching the critical bonding pressure. However, the excessive bonding pressure inversely increased the connection resistance of ACF interconnection.

About the conductive particles content, if more conductive particles were added, the connection resistance rapidly decreased and then became constant. This is because the counter-effect of two opposing factors, the resistance increase by a decrease of contact area per one particle and the resistance decrease by increasing number of conduction path. In addition, environmental effects on contact resistance and adhesion strength such as thermal aging, high temperature/humidity aging and temperature cycling were also investigated.

As a whole, better design of ACF materials can be achieved by understanding the ACF conduction mechanism.

1. Introduction

Recently LCD panels became very important components for portable electronics. The requirements for better resolution and color quality LCD panels need an advanced LCD packaging technology because of higher numbers of pixels and I/Os. to be interconnected. Therefore anisotropic conductive films (ACFs) used to connect the output lead electrode of the tape automated bonding (TAB) (which is mounted to the driver IC) to the transparent indium tin oxide (ITO) electrode of the LCD panels became important as a high density interconnection material [1]. ACFs are

generally composed of an adhesive polymer matrix and a fine conductive filler using metallic particles or metal-coated polymer balls. Connecting with ACF forms electrical and mechanical contact in which the connection resistance is higher than that of soldering and bonding temperature lower than those that result from soldering and much finer pitch conduction pads can be interconnected simultaneously using ACFs than solders. Intensive research and development work has been carried out in the field of Flip-chip and Chip-On-Glass technology using ACF as an alternative of soldering [2-3]. The electric current passing through electrical conductive particles in ACF becomes dominant conduction paths and the role of conductive particle is to keep electrical conductivity low [4]. Conduction joints between the particles and the conductive surfaces are constructed by the elastic/plastic deformation of conductive particles with applied pressure. Therefore the electrical resistance of ACF depends on the external pressure, mechanical and electrical properties of particles [5-7]. Few studies have been performed on the pressure engaged electrical conduction mechanism of ACF materials. Understanding the conduction mechanism of ACFs will impact on the better performance and reliability of LCD packages by choosing right ACF materials, proper processing conditions and ACF materials development in the future.

In this study, we examined the effect of bonding pressure on the electrical conductivity of ACF's with variations of number, diameter, hardness and electrical properties of conductive particles using elastic deformation model and finite-element method (FEM). The relationship between the ball contact area and the applied pressure was investigated, and correlated with contact resistance. For the experimental verification, we investigated the effect of the bonding pressure on the electrical resistance, adhesion strength and reliability of ACF interconnection using Ni particles and Au-coated ball-filled ACFs. Conductive particle content were also varied to find out the optimum ACF design condition.

2. Derivation of the model

2.1 Analytical model

Electrical conduction is made within the ACF by a mechanical contact of conductive particles and pads. Current flowing through the contacts developed is constricted because of the small contact area developed between particles and pads. The bending of the current-flow paths requires an added voltage called the constriction voltage. Furthermore, additional voltage may be required to force current through a

high-resistance film that may be separating two conductors, such as oxide film.

The contact resistance, R_c is expressed like this.

$$R_c = R_{CR} + R_f \quad (1)$$

where R_{CR} is the resistance due to constriction and R_f is the film resistance. For contacting materials that form metal to metal contacts R_f is negligible. However, the film resistance is higher than expected where there is an oxide film or entrapped organic film between the conducting surfaces. Therefore the film resistance contribution to contact resistance could be a function of metal surface condition and the organic adhesive used.

The constriction resistance R_{CR} , has been shown to be

$$R_{CR} = (\rho_1 + \rho_2) / 2d \quad (2)$$

where ρ_1 , ρ_2 are the intrinsic resistivity of metal conductive particles and substrate, and d is the diameter of the contact spot area [6]. The contact spot area, $a = \pi d^2/4$ for circular contact spots, must be a function of the applied pressure on conductive particles and the amount of deformation that occurs as a result of the applied pressure.

The magnitude of the deformation for a given pressure is determined by number, the contact hardness and the diameter of conductive particles. In considering these factors, the radius of contact area between conductive particles with number of N and flat substrate under applied force F , can be obtained using an elasticity theory [8].

$$d = \left(\frac{3FR}{4NE^*} \right)^{1/3} = 1.44 \left(\frac{FD}{NE^*} \right)^{1/3} \quad (3)$$

$$\frac{1}{E^*} = \frac{1 - \nu_p^2}{E_p} + \frac{1 - \nu_s^2}{E_s}$$

where D and R are the diameter and radius of curvature of conductive particles, E is the elastic modulus, ν the poisson's ratio, p and s the particle and substrate, respectively. From Eq.(3) the contact area becomes

$$a = 1.63 \left(\frac{FD}{NE^*} \right)^{2/3} \quad (4)$$

Substituting Eq.(4) into Eq.(2) gives

$$R_{CR} (\text{elastic}) = 0.347 (\rho_1 + \rho_2) \left(\frac{NE^*}{FD} \right)^{1/3} \quad (5)$$

The intrinsic resistance of an individual particle may be estimated assuming an equivalent cross-sectional area of

sphere, that is, the cross-sectional area of a cylinder whose volume is equal to the sphere with diameter of D . By geometry, this cross-sectional area can be explained to be $0.524D^2$. The intrinsic resistance leads to the relation [9].

$$R_i = \rho_i \left(\frac{D}{0.524D^2} \right) = \frac{\rho_i}{0.524D} \quad (6)$$

In ACF interconnection the interconnection resistance is also function of the number of conduction paths N between electrodes.

According to the schematics of ACF interconnection in Fig.1, the resistance may be described as this.

$$R_c = R_e + R_e' + \frac{2R_{CR} + R_i}{N} \quad (7)$$

where R_e and R_e' are the resistance of two electrodes, R_{CR} the particle-electrode contact resistance, R_i the resistance across one particle, N the number of conduction paths. If a four-point-probe resistance measurement is used, R_e and R_e' is eliminated from Eq. (7).

Substituting Eq.(5), (6) into Eq.(7) yields

$$R_c = \frac{0.69 (\rho_1 + \rho_2) \left(\frac{NE^*}{FD} \right)^{1/3} + \frac{\rho_i}{0.524D}}{N} \quad (8)$$

This describes interconnection resistance of ACF in terms of sample geometry, particle size, applied pressure, and the intrinsic properties of the conductive particles; this is for elastic deformation of conductive particles.

2.2 Finite Element Model

The above models are derived for the use of anisotropic materials assuming elastic deformation of the spherical conducting particles or substrates. However, these models contain several simplifying assumptions. For significant plastic deformation cases such as a soft substrate with hard conducting particles or metal-coated polymer spheres with a hard substrate material, the analytical model for small deflections of conductive sphere are no longer valid. Therefore, finite element models(FEM) of the contact have been constructed using the ANSYS program to explore the effect of the large deformation of conductive particles or soft substrate on contact resistance of the ACF joint.

Two large deformation cases can be considered. One is the joint with significant plastic deformation of the substrate and the other is the case of the sphere. Fig.2(a) and 2(b), respectively illustrate the plastic deformation of metal-coated polymer sphere and the significant plastic deformation of soft substrate, for example, copper conductor contacted with hard nickel sphere. Where the compression load is applied to the conductive sphere, the growth of the contact area is achieved by the flatness of sphere on hard substrate and the sphere

indentation on a soft substrate

Fig.3 shows the FEM meshes of soft conductive sphere on a hard substrate and the indentation of a hard sphere on a soft substrate. We assume that the substrate in Fig.3(a) and the sphere in Fig.3(b) are rigid bodies. The sphere and soft substrate exhibit nonlinear large deformation behaviour when being applied by a compressive load up to 1N. Material used in this calculation are considered as almost incompressible body for the incremental nonlinear analysis of plastic deformation [10]. Four-node mixed hyper-elastic solid elements and 2-D point-to-ground contact elements were adopted in this calculation. We used the material constants listed in Table I.

Assuming that the nodal point displacements of the finite element mesh completely specify the displacement in the body, we calculated the increment of contact area between the conductive sphere and substrate for each case and converted them into contact resistance from Eq.(3).

3. Experimental verification

3-1. ACF material

ACF used in this study is 20~30 μm in thickness and made of insulative resin in which nickel and gold-plated polymer particles dispersed. Seven kinds of ACF with different contents of gold-plated polymer particles were prepared to investigate the effects of conductive filler content on contact resistance of ACF interconnection. Adhesive resins prepared by formulating epoxy resin, curing agents and flexibilizing agents were converted to a dry film format for easy handling. The adherends of ACF interconnection are a dummy ITO glass with surface resistance of 50~70 $\Omega/\text{sq.}$ and polyimide flexible film with corresponding patterned metallization pads. The metal pad on flexible film consists of approximately 35 μm thick copper, electrolytically plated 2 μm nickel and 0.5 μm gold on top. Terminals were arranged in 200 μm pitches and the size of terminal connected with ACF was 100 μm wide and 3 mm long.

3-2. Bonding Process

ACFs were cut to the correct size to cover the bonding area and were first pre-bonded to the flexible film using light pressure and at the same time applying heat(80 $^{\circ}\text{C}$, 1.5kg/cm² for 5 s). After the pre-bonding the carrier film was removed and then flexible film with pre-bonded ACF was final bonded to the ITO glass substrate. The bonding parameters are shown in Table II.

For evaluation of ACF interconnection, connection resistance and adhesion strength between flexible film and ITO glass were measured. To investigate the relation of connection resistance and bonding pressure, various bonding pressures were applied. The connection resistance was measured by a four-point probe method and adhesion strength by 90 $^{\circ}$ peel strength measurement. After bonding, the cross-section of bonded area was observed by a scanning electron microscopy (SEM). The peel strength test was carried out on INSTRON

static model 4206 with a cross-head speed of 0.1 mm/min.

For reliability test of ACF interconnection, three environmental tests were carried out. 125 $^{\circ}\text{C}$ temperature aging test and high temperature/humidity test in 85 $^{\circ}\text{C}$ /85%RH condition were performed during 500 hours. -40 to 85 $^{\circ}\text{C}$ temperature cycling test was carried out in Thermotron 2800 for 250 cycles. Also contact resistance and peel strength were measured after each test.

4. Results and discussions

4-1. Analytical model

Fig. 4 shows the contact resistance vs. load relationship from analytical method. Increasing the load reduces the contact resistance. The effect of number of conducting particles on contact resistance is shown in Fig. 4(a). The larger the number of conductive particle in ACF is, the less the contact resistance becomes. When the ACF with N particles is used, the load applied to one particle becomes 1/N compared with a particle, and the deformation of particles becomes less and the contact resistance should increase for each particles. However as shown in Fig. 4(a), the influence of electrical resistance reduction caused by N conductive particles is greater than electrical resistance increases due to 1/N load applied to each particles.

Fig.4(b) show the contact resistance of metal-coated polymer balls compared with that of metal particles. Large contact resistance is obtained for metal-coated polymer balls because of the current flowing only at the skin area of particles. And Fig. 4(c) show the effect of coated material on contact resistance. Also, Fig.4(d) shows that contact resistance decreases with increasing diameter of conductive particles.

The analytical model predicts that the contact resistance decreases with increasing number of conductive particles and particle size, and intrinsic conductivity. Thus to produce the highly conductive interconnection using ACF, it is necessary to choose relatively soft, large particle size and high conductive material for the conductive particle.

4-2. FEM Model

Fig. 5 shows the FEM results of the conductive particle deformation process under compressive load of 100 gram force. The deformed mesh patterns and stress distribution during deformation process are represented in Fig. 5(a), and the calculated contact area and contact resistance are shown in Fig. 5(b) and 5(c), respectively. In this case, the conductive sphere is Au-coated polymer ball of 40 μm diameter and the substrate indium-tin-oxide (ITO) coated glass.

The amount of deformation (AD) and the compressive load are numerized under figures (i) to (iii). A compressive load of 134.6 gram force in the amount of deformation over 50%. As can be seen in Fig.5, the center of the conductive sphere is compressed more largely. Fig. 5(b) shows the relationship between compressive load and contact area. Increasing the contact area between conductive sphere and substrate leads to the decrease of the contact resistance according to Fig. 5(c).

This numerical results suggests that the load near 100 gmf is obviously a minimum load at which the sufficiently low contact resistance can be obtained for one conductive particle. Fig. 6 show the numerical results of the contact area and contact resistance behaviour for the contact process of 40 μm Ni particle indentation on soft Cu substrate. As pressure increases, contact area increases, and a sharp decrease of contact resistance is followed by a constant resistance value.

4-3. Effect of bonding pressure

Figure.7 shows the relationship between connection resistance and bonding pressure for an ACF with Ni particles and Au-coated polymer sphere. Both ACF interconnection indicate connection resistance of below 0.6 Ω in region of more than 3kgf/cm² bonding pressure and the connection resistance of Ni-filled ACF is lower than that of Au-coated polymer sphere-filled ACF. However, at 2kgf/cm² the connection resistance and standard deviation of Ni-filled ACF interconnection which are higher than that of Au-coated polymer sphere-filled ACF. In ACF interconnection, as bonding pressure increase, the interconnection width between metallization pads and glass substrate decrease, therefore the amount of particle deformation increase. An increase in contact area of conductive particles decreased the interconnection resistance further.

Another interesting observation is minor increase of resistance after 3kgf/cm². This is presumable to the bouncing effect of the epoxy resin after the pressure release. Fig.8 shows the cross-sections of the deformed conductive Au-coated polymer sphere and corresponding contact area as a function of bonding pressures.

This behaviour of conductive sphere deformation under ACF bonding process is phenomenologically in good agreement with the simulation explained previously. Metal-coated polymer particles at 5 kgf/cm² were almost flattened and the metallization pads were in direct contact with the glass substrate. This is because Au-coated polymer sphere is much softer than Ni particle.

As a result of over-pressure, high contact resistance due to a separation of surface gold layer or cracks is observed, and becomes a disadvantage of Au-coated polymer sphere-filled ACF [2]. But Au-coated polymer sphere may induce less internal stress than Ni particle. ACF with hard Ni particle may induce elastic stress which can lead to a resistance increase or an open circuit in reliability test when applied excessively high bonding pressure [11].

4-4. Effect of particle content

Fig.9 shows the relationship between particle content of ACFs and the connection resistance. There is a linear relationship between particle content of ACFs and the density of the particle in ACF. For ACFs with initial particle contents increase, the number of particles on the terminal increases and the connection resistance decreases. However, over the 4wt% of conductive particles, the connection resistance does not decrease further, but becomes stabilized. As conductive particle content increase, the connection resistance decrease

because of more conductive paths. However, when an ACF with more particle content is interconnected at a constant pressure, the pressure applied to one particle becomes less than an ACF with a smaller particle content at the same pressure. Therefore, the deformation of each particle becomes less resulting in a smaller contact area. For this reason, the connection resistance can increase, although more particle content is added. At smaller particle content region up to 4wt%, resistance decrease by more conductive path becomes more dominant. But after the content of conductive particle is over 4wt%, the connection resistance becomes stabilized, because two opposing factors affect each other.

4-5. Reliability

Fig.10 shows the contact resistance changes at various bonding pressures after the completion of three environmental tests. The x-axis represents contact resistance and the y-axis represents a normal probability scale. The slope of the straight line fit is the standard deviation. The contact resistance and standard deviation increased after all three tests. Among these, 85 $^{\circ}\text{C}$ /85 RH test, in particular, caused a significant effect on the degradation of the ACFs conducting performance compared with 125 $^{\circ}\text{C}$ aging test and temperature cycling test. In addition, the mean contact resistance of Ni-filled ACF is higher than that of Au-coated polymer sphere-filled ACF interconnection. For Ni-filled ACF interconnection with starting at a mean contact resistance of 0.771 Ω , 85 $^{\circ}\text{C}$ /85 RH exposure increases to 178 Ω and produces 15 open joints. In contrast for Au-coated polymer-filled ACF, start with 0.718 Ω and increases to 21.44 Ω and results in one open joint. The figure also indicates that at the same conditions, Ni-filled ACF interconnection is less reliable than Au-coated polymer-filled ACF interconnection. This difference in the increased contact resistance between Ni-filled ACF and Au-coated polymer sphere-filled ACF is presumably due to the difference in the coefficient of thermal expansion(CTE) of conductive particles used. From Table. III, the CTE of Ni particle is obviously much smaller than that of Au-coated polymer sphere that is similar to that of cured thermosetting epoxy-based adhesive. If thermal expansion of epoxy adhesive is larger than that of conducting particle, especially to the thickness direction, the interconnection gap will occur. If the conducting particle does not expand as the matrix does. This will result in a contact resistance increase.

Fig.11 shows the microstructure of ACF joint after each reliability test. The conduction gap is not found at the completion of 125 $^{\circ}\text{C}$ aging test and temperature cycling test. However, the formation of conduction gap is obviously appeared after 85 $^{\circ}\text{C}$ /85%RH test as indicated by an arrow. During 85 $^{\circ}\text{C}$ /85%RH test, the humidity causes hygroscopic expansion of epoxy and weakening of epoxy/contact pad adhesion both resulting in a contact resistance increase. The another factor for the increasing electrical resistance is the oxidation of metallic filler [11-12] which was observed from Electron Probe Micro-Analysis(EPMA) studies on a

cross-sectioned joint of catastrophic conduction failure after a temperature humidity test. Fig. 12 show the distribution of O, Ni, C, Cu, and Au both on the Ni-filled ACF interconnection by EPMA element mapping. The presence of oxygen and carbon comes from epoxy adhesive layer. In particular, the presence of oxygen without carbon on the contact interface between Ni particle and Cu/Ni/Au metallization pad suggests the Ni oxide formation which may degrade the electrical contacts resulting in an increase of contact resistance. It is unlikely that this oxide illustrated in Fig. 12(b) originated from the surface of metallization pad, because this pad surface is electroplated with a thin gold layer less in Fig. 12(f). The peel strength measurement result after three environmental tests were given in Fig. 13 showing 17%, 160% increase after temperature cycling test and high temperature aging test, and 62% decrease after temperature humidity test. Fractures generally occurred at the metallization pad/adhesive interface after environmental exposure. The peel strength variation of ACF interconnection was not dependent on the kind of conductive particles, but dependent on the property of adhesive layer. Decrease of peel strength was mainly by the temperature humidity exposure, probably the absorbed moisture can degrade the adhesion properties of adhesive layer. Increase of peel strength after temperature aging tests and temperature cycling may be attributed to full-cured epoxy during heating.

5. Conclusion

We have discussed the conduction mechanism of ACF interconnection for LCD packaging applications. Analytical models with the consideration of elastic deformation of contact material were used to evaluate the several factors of electrical contact, and FEM was used to investigate the electrical conduction through the large deformation of conductive particles or conductor substrate. Electric properties, and the reliability of ACF interconnection were investigated using 5 μ m diameter Ni-filled ACF and Au-coated polymer-filled ACF. Several results can be summarized as follows.

1. Electrical conduction through the pressure engaged contact area between conductive particles and substrate is the main conduction mechanism in ACF interconnection.
2. The bonding pressure plays an important role in the electrical properties of ACF interconnection with pressure dependent conduction mechanism. In general, as bonding pressure increases, a sharp decrease of contact resistance followed by a constant value are observed after reaching the critical bonding pressure.
3. Contact resistance of ACF is determined by the contact area change between particles and contact substrate. Therefore the number, the size, and the hardness of electrical conductive particles are important variables as shown in simulated results.
4. From the experimental verification, the model was found to be phenomenologically in good agreement with experimental results except higher bonding pressure realm. The excessive

bonding pressure inversely increased the connection resistance of ACF interconnection, presumably due to the bouncing effect of the epoxy resin after the pressure release or due to the separation of surface gold layer on the flattened polymer sphere.

5. When more conductive particles are added, the connection resistance rapidly decreased and then became constant. This is because the counter-effect of two opposing factors, the resistance increase by a decrease of contact area per one particle and the resistance decrease by increasing number of conduction path.

6. From reliability test, the Ni-filled ACF interconnection bonded with high bonding pressure was less reliable than the Au-coated polymer sphere-filled ACF. Thermal stress from CTE mismatches between conductive particle and adhesive and elastic stress from the excessive pressurization could be the two of the main factors. Increasing contact resistance after temperature humidity test is also due to the oxidation of metal conductive particles. Peel strength decreased due to the degradation of adhesion of adhesive layer by the moisture attack after the temperature humidity exposure.

References

- [1] S. Asai et al., "Development of an Anisotropic Conductive Adhesive Film (ACAF) from Epoxy Resins," *J. of Appl. Polym. Sci.* 56, 769-777 (1995)
- [2] H. Date et al., "Anisotropic Conductive Adhesive for Fine Pitch Interconnections," *Proc., International Symposiums on Microelectronics '94*, 570-575 (1994)
- [3] A. Torri, M. Takizawa, and K. Sasahara, "Development of Flip Chip Bonding Technology using Anisotropic Conductive Film," *Proc., 9th International Microelectronics Conference*, 324-327 (1996)
- [4] M. Mizuno, M. Saka, and H. Abe, "Mechanism of Electrical Conduction Through Anisotropically Conductive Adhesive Films," *IEEE Trans. on Compon., Packag. Manuf. and Tech., Part A*, 19, 546-553 (1996)
- [5] K. Kulojarvi, P. Savolainen, and J. Kivilahti, "Bonding Flexible Circuits and Bare Chips with Anisotropic Electrically Conductive and Non-conductive Adhesives," *10th European Microelectronics Conference*, 28-34 (1995)
- [6] R. Holm, *Electric Contacts*, Springer Verlag, New York, 1981, pp.45
- [7] Y. Wei, and E. Sancaktar, "A Pressure Dependent Conduction Model for Electrically Conductive Adhesives," *Proc., International Symposiums on Microelectronics '95*, 231-236 (1995)
- [8] K. L. Johnson, *Contact Mechanics*, Cambridge University Press, Cambridge, 1985, pp.85-106
- [9] G. R. Ruschau, S. Yoshikawa and R. E. Newnham, "Resistivities of Conductive Composites," *J. of Applied Physics*, 72, 953-959 (1992)
- [10] T. Sussman and K. J. Bathe, "A Finite Element Formulation for Nonlinear Incompressible Elastic and Inelastic Analysis," *Computers & Structures*, 26, 357-409 (1987)
- [11] J. Liu and R. Rorgren, "Joining of displays using

Thermosetting Anisotropically Conductive Adhesives", J. of Elec. Manuf., 3, 205-214(1993)
 [12]J. Liu, K. Boustedt and Z. Lai, "Development of Flip-chip Joining Technology on Flexible Circuitry using Anisotropically Conductive Adhesives and Eutectic Solder", Proc. of Tech. Prog., SMI, 102-109(1995)

Acknowledgements

The authors appreciate the help of Dr. I. Y. Kim and I. Y. Jeong of KOLON research center for useful discussions and experiment. This work had been supported by the KOLON under Grant No. GI28650.

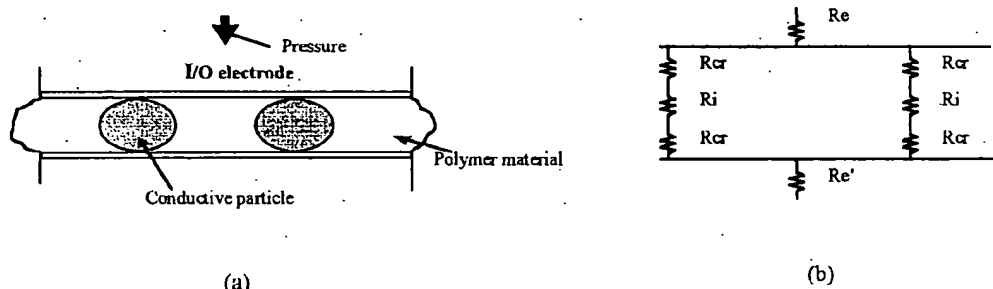


Fig. 1 (a) Schematics of ACF interconnection and (b) equivalent resistor chain.

Table. 1 Material Properties Used In Analysis

	Cu on FR-4	Ni	Ni-coated polymer ball	Au-coated polymer ball	ITO glass substrate
E (GPa)	129.8	199.5	2.5	2.5	-
resistivity (Ωm)	1.8×10^{-8}	8×10^{-9}	$*1.56 \times 10^{-7}$	$*4.16 \times 10^{-8}$	1.89×10^{-6}
Poisson's ration	0.343	0.312	0.4	0.4	-

* Resistivity of metal-coating layer

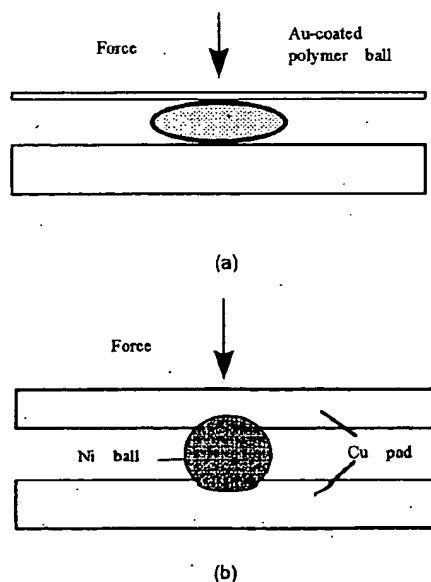


Fig. 2 Schematic illustrations of (a) deformation of metal-coated polymer ball and (b) indentation of Ni particle into Cu pad.

BEST AVAILABLE COPY

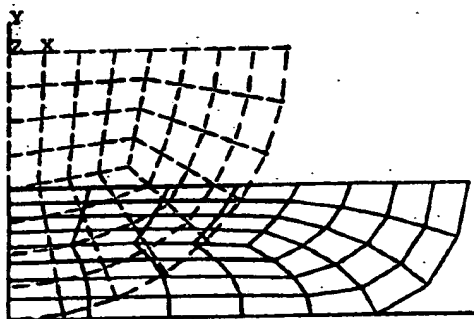


Fig. 3(a) FEM mesh of conductive sphere with initial and deformed shape.

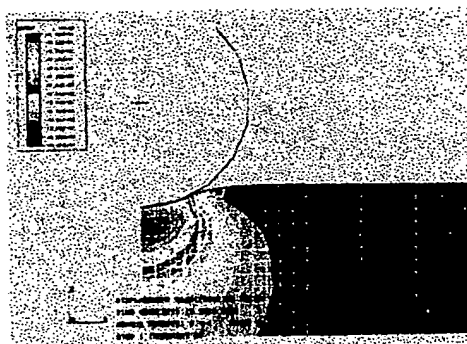
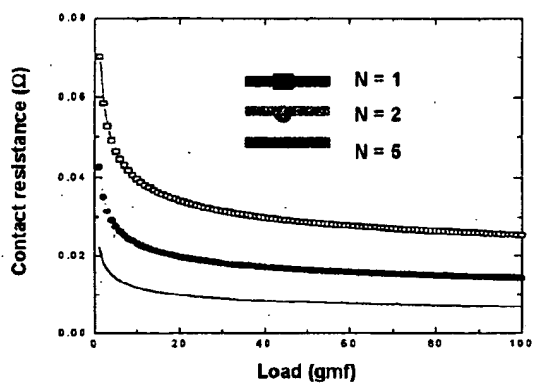
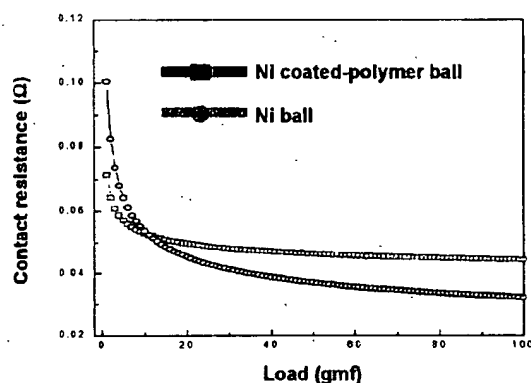


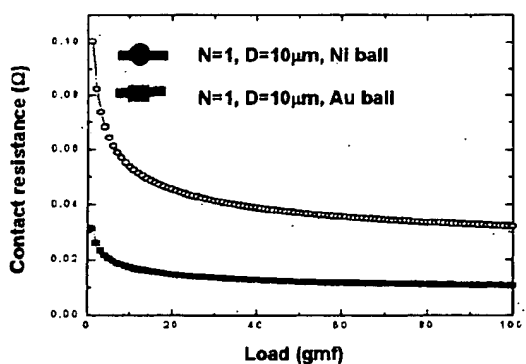
Fig. 3(b) FEM mesh of indentation with hard sphere on Cu substrate.



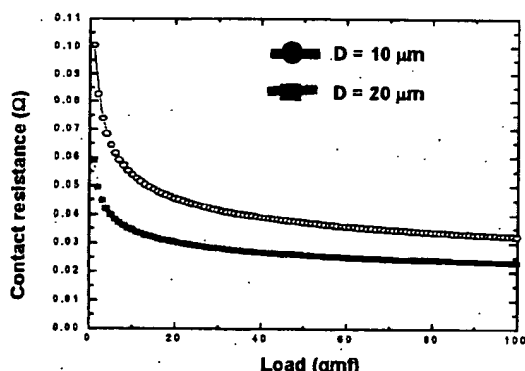
(a)



(b)



(c)



(d)

Fig. 4 Contact resistance vs. Load results from analytic method showing the effect of (a) number of conducting particles, (b) metal-coated polymer ball, (c) conducting material and (d) ball diameter.

BEST AVAILABLE COPY

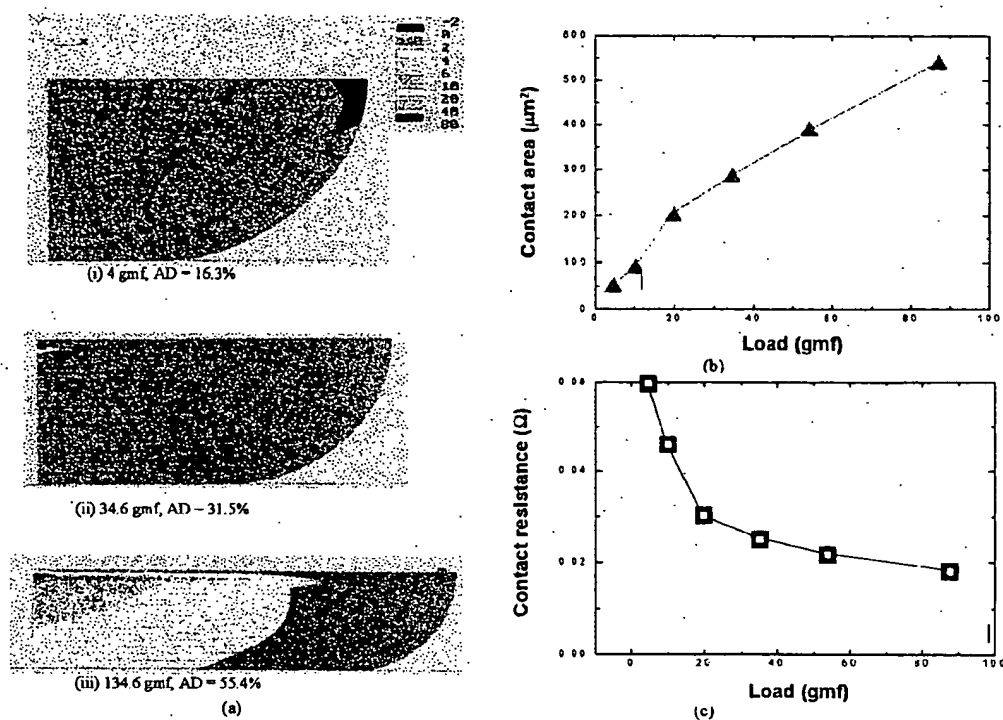


Fig. 5 Results of conductive ball deformation process by FEM. (a) ball deformation process and stress distribution, (b) applied load vs. contact area, (c) applied load vs. contact resistance.

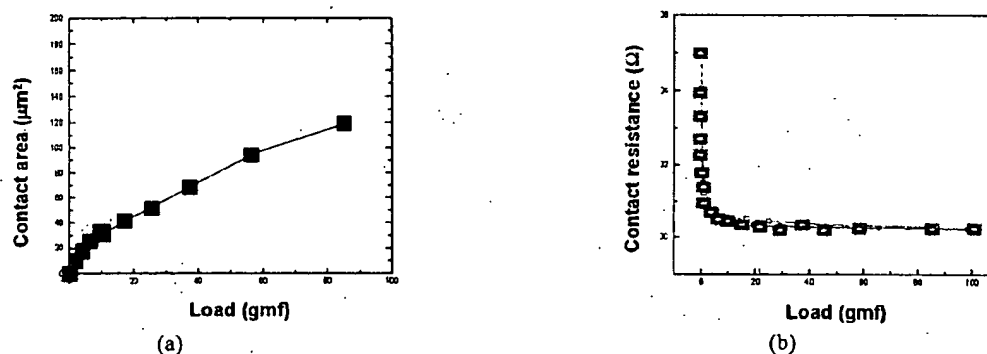


Fig.6 Results of Ni ball indentation on Cu substrate by FEM. (a) applied load vs. contact area and (b) load vs. contact resistance.

Table. II The Bonding Parameter for ACF bonding

Pre-bonding of FPC to glass substrate	
Temperature($^{\circ}\text{C}$)	80
pressure(kgf/cm^2)	2
Time (s)	5
Final bonding of FPC to glass substrate	
Temperature($^{\circ}\text{C}$)	180
Pressure(kgf/cm^2)	1.5, 2, 3, 4, 5
Time (s)	20

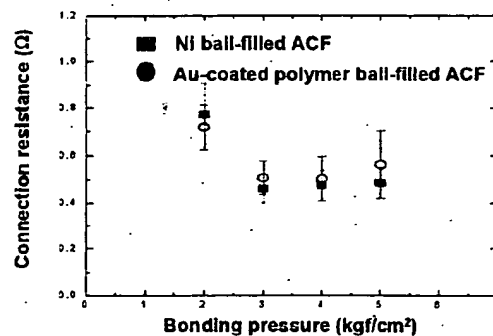


Fig. 7 Connection resistance plotted as a function of bonding pressure

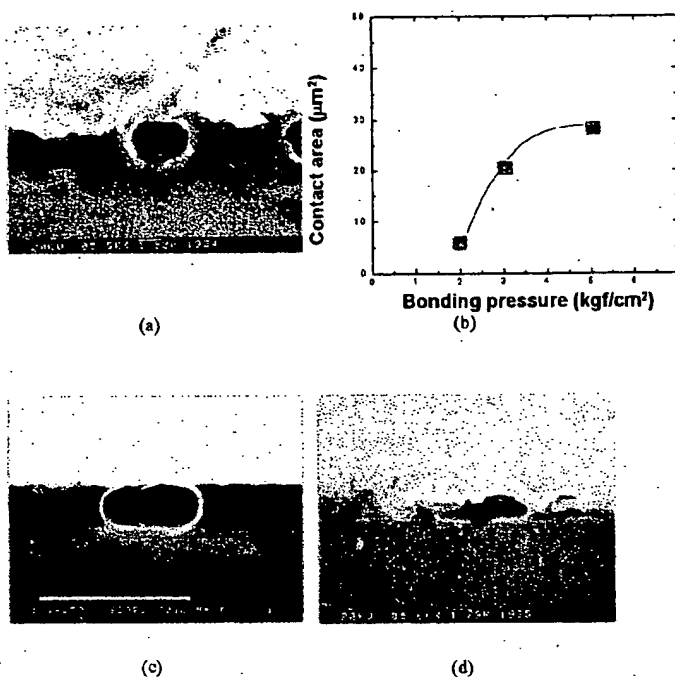


Fig. 8 The cross section of Au-coated polymer sphere deformed under pressure (a) 2kgf/cm², (c) 3kgf/cm², (d) 5kgf/cm² and (b) contact area

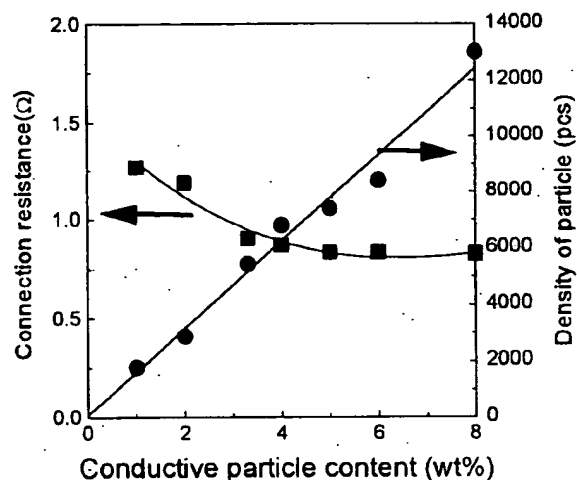


Fig. 9 Connection resistance vs. number of conductive particle content in ACF (wt%)

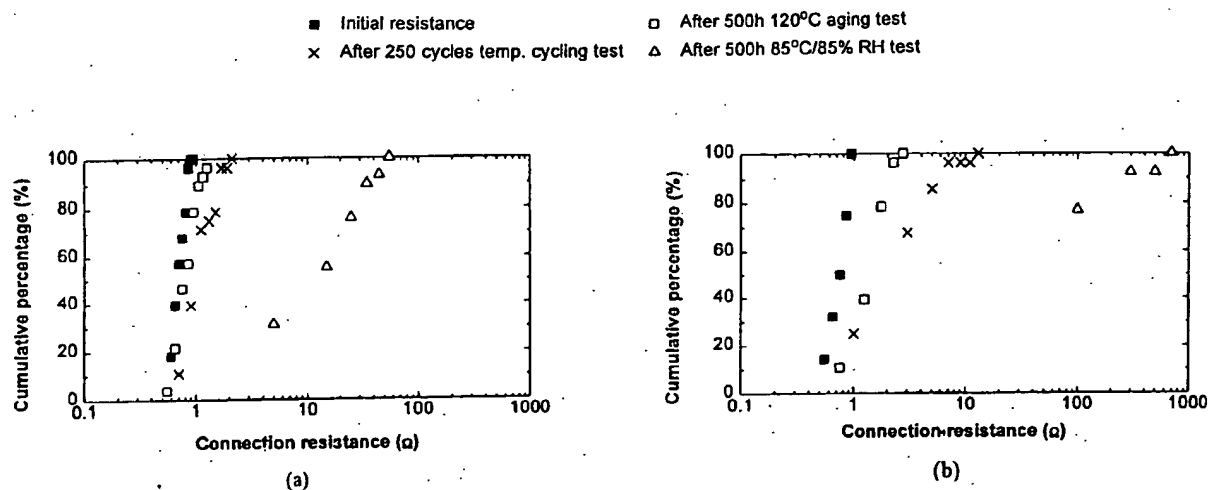


Fig. 10 The connection resistance distribution of initial and at the completion of the three reliability tests : bonding pressure is 2kgf/cm² (a) Au-coated polymer sphere-filled ACF and (b) Ni-filled ACF.

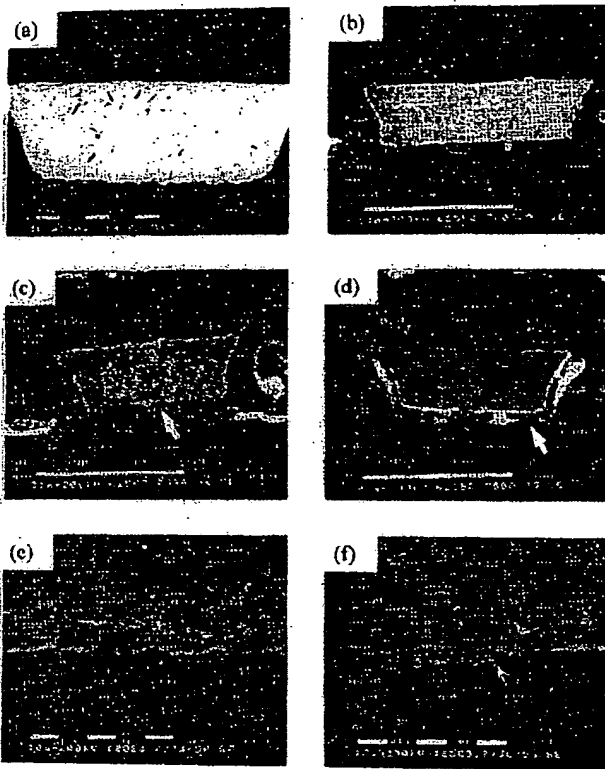


Fig. 11 Microstructure of ACF joint after (a), (b) 125 °C aging test, (c),(d) 85 °C/85%RH test and (e),(f) temperature cycling test. The arrow in (c), (d) indicate the conduction gap.

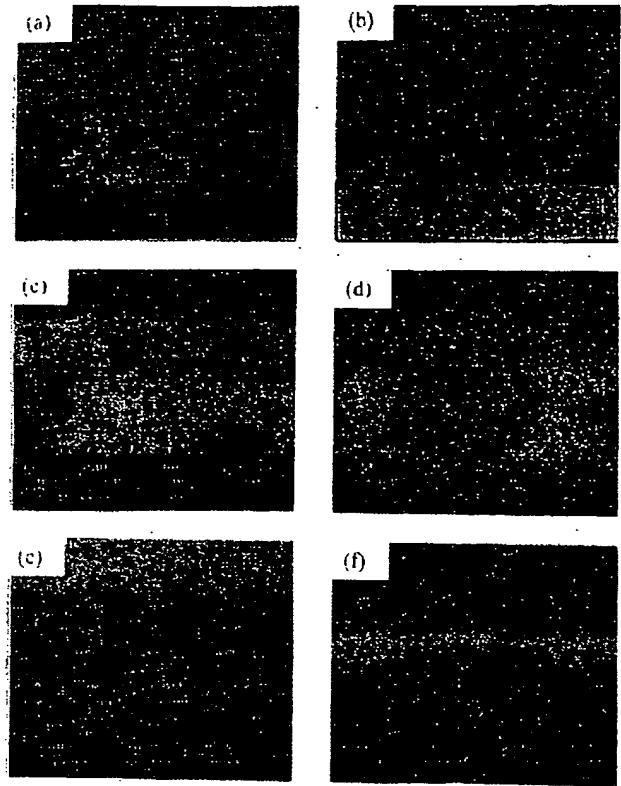


Fig. 12 (a) EPMA micrographs of Ni-filled ACF interconnection after 500 h, 85 °C/85%RH test, EPMA mappings of (b) oxygen, (c) nickel, (d) carbon, (e) copper and (f) gold.

Table. III CTE's of metal and adhesives

Coefficient of thermal expansion ($10^{-5}/^{\circ}\text{C}$)					
Conductive particle				Adhesive	
Ni	Cu	Au	Metal-coated polymer	Thermoplastic	Thermosetting
1.3	1.7	1.4	7.0	12	7.9

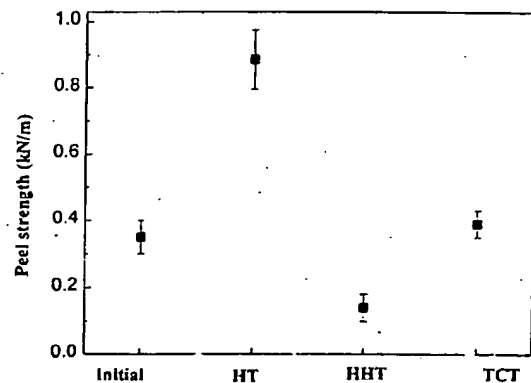


Fig. 13 Peel strength variation between before and after the reliability tests. (HT: High Temperature aging test, HHT: Hot Humidity Test, TCT: Temperature Cycling Test) Initial sample condition: 3 kgf/cm², 180 °C, 20 sec.